

## BACTERIAL AND PROTEIN ADHESION ON NI-P-PTFE COATED SURFACES

Q. Zhao, C. Liu, Y. Liu and S. Wang

Division of Mechanical Engineering & Mechatronics, University of Dundee  
Dundee DD1 4HN, UK Email: Q.Zhao@dundee.ac.uk

### ABSTRACT

The adhesion of bacteria and proteins on the surfaces of heat exchangers and food processing equipment has been recognized as a widespread problem. Biofouling not only reduces heat transfer performance significantly, but also causes considerable pressure drop, calling for higher pumping requirements. Biofouling also present a considerable hygiene risk in the food industry. It would be much more desirable if surfaces with an inherently lower stickability for biofouling could be developed. In this paper, stainless steel 304 plates were modified by electroless plating Ni-P and small amounts of PTFE. The experimental results showed that the surface free energy of the Ni-P-PTFE coatings, which were altered by changing the PTFE content in the coatings, had a significant influence on the adhesion of bacterial, protein and mineral deposits. The Ni-P-PTFE coatings reduced the adhesion of these deposits significantly. The anti-fouling mechanism of the composite coatings was explained with the extended DLVO theory.

### 1. INTRODUCTION

Biofouling has been recognized as a widespread problem in design and operation of processing equipment such as heat exchangers, cooling water systems and food processing equipment (Lalande et al., 1989 and Notermans et al., 1991). Biofouling does not only present a considerable hygiene risk in the food industry, but also causes economic losses. The rapid development of the global offshore industry and of amphibious chemical, steel and power plants leads to more intensive use of seawater as a cooling medium. However pipelines and heat exchangers using seawater as coolant suffer from biological fouling (Lucas et al., 1996 and Koh et al., 1991). Biofouling not only reduces heat transfer performance significantly, but also causes considerable pressure drop, calling for higher pumping requirements. For example, biofouling on a 20-cm carbon steel pipe reduced the cross-sectional area by 52% in 2.5 years (Gaffoglio, 1987). The cost of cleaning and lost output can be extremely high. In addition to biofouling, crystalline fouling also occurs in heat exchangers using seawater as a coolant (Ritter and Suitor, 1975). Calcium carbonate, calcium sulphate or other salts that have solubility that diminishes with increasing temperature can form on exchanger tubes as crystalline deposits. Biofouling

and crystalline fouling may occur singly or in combination depending on the operating parameters.

An effective and desirable approach to reduce fouling is to alter the surface properties of the equipment and to make it less attractive for the fouling components, so that they can be removed easily from the surfaces by flowing water. Many attempts have been made to reduce fouling by coating surfaces with PTFE due to its non-stick properties. However, the poor thermal conductivity, poor abrasion resistance and poor adhesion to metal substrate of the PTFE coatings currently inhibit their commercial use (Müller-Steinhagen and Zhao, 1997). The first electroless Ni-P-PTFE composite coatings were introduced in 1980 (Tulsi, 1983). The incorporation of PTFE nanoparticles into the Ni-P matrix can take advantage of the different properties of Ni-P alloy and PTFE. The resulting properties of electroless Ni-P-PTFE coatings, such as non-stick, higher dry lubricity, lower friction, good wear and good corrosion resistance, have been used successfully in many industries. Because the electroless Ni-P-PTFE coatings are metal-based, their thermal conductivity, anti-abrasive property, mechanical strength and adhesion strength to the substrate are superior to standard PTFE coatings. In this paper, stainless steel 304 plates were coated with Ni-P-PTFE with various PTFE content. The effect of surface energy on the adhesion of bacteria, protein and mineral deposits were investigated.

### 2. EXPERIMENTAL PROCEDURE

#### 2.1 Ni-P-PTFE composite coatings

In this investigation, the stainless steel 304 sheets of 10mm × 15mm × 0.35mm, stainless steel heater rods with 10 mm in diameter and q-sensor discs with 10 mm in diameter were coated with Ni-P-PTFE. To improve coating adhesion and corrosion resistance, graded Ni-P//Ni-P-PTFE layers were coated on the stainless steel substrates. The interlayer thickness of Ni-P was 1 μm. The Ni-P-PTFE composite coating was prepared by gradually increasing the PTFE content from the Ni-P interlayer to the top surface. Since there was no obvious interface between the coatings, the coating adhesion was improved significantly. The stainless steel samples were first cleaned with alkaline solution at 60–80°C for 10–20 minutes and then rinsed with water.

They were dipped into a dilute HCl solution (1 M) for 30 s and then rinsed with cold water and deionized water, respectively. The composition of electroless Ni–P–PTFE solutions used in this investigation included 25 g/l NiSO<sub>4</sub>·6H<sub>2</sub>O; 25 g/l Na<sub>3</sub>C<sub>6</sub>H<sub>5</sub>O<sub>7</sub>·2H<sub>2</sub>O; 30 g/l NaH<sub>2</sub>PO<sub>2</sub>·H<sub>2</sub>O; 18 g/l NaCH<sub>3</sub>COO; 0–18 ml/l PTFE (60 wt.%) and 0–0.6 g/l cationic surfactant. A 60% PTFE emulsion from Aldrich with a particle size in the range 0.05–0.5 μm and a cationic surfactant were diluted with deionized water and stirred with a magnetic stirrer for 1 hour. Then the suspension was filtered with a filter of pore size 0.2 μm before use. PTFE particles in the baths were dispersed uniformly by the surfactant without using any mechanical agitation or ultrasonic homogeniser. The coating thickness (about 10 μm) was measured using a digital micrometer and the coating compositions were analysed with an energy dispersive X-ray microanalysis (EDX) model JEOL T-300 at beam energy of 20 keV. The surface morphology of the coatings was analysed with a scanning electron microscope (SEM).

## 2.2 Contact angle measurements

Prior to contact angle measurement, samples were ultrasonically cleaned in acetone, ethanol and deionized water in sequence. Contact angles were obtained using the sessile drop method with a Dataphysics OCA-20 contact angle analyser. This instrument consists of a CCD video camera with a resolution of 768×576 pixel and up to 50 images per second, multiple dosing/micro-syringe units and a temperature controlled environmental chamber. The drop image was processed by an image analysis system, which calculated both the left- and right contact angles from the shape of the drop with an accuracy of ± 0.1°. Three test liquids were used as a probe for surface free energy calculations: distilled water, diiodomethane (Sigma) and ethylene glycol (Sigma).

## 2.3 Surface free energy

The theory of contact angle of pure liquids on a solid was developed 200 years ago in terms of the Young equation (Young, 1805):

$$\gamma_L \cos \theta = \gamma_S - \gamma_{SL} \quad (1)$$

where  $\gamma_L$  is the experimentally determined surface tension of the liquid,  $\theta$  is the contact angle,  $\gamma_S$  is the surface free energy of the solid and  $\gamma_{SL}$  is the solid/liquid interfacial energy. van Oss et al. (1988) developed an acid-base approach for the calculation of surface free energy. The surface free energy is seen as the sum of a Lifshitz-van der

Waals apolar component  $\gamma_i^{LW}$  and a Lewis acid-base polar component  $\gamma_i^{AB}$ :

$$\gamma_i = \gamma_i^{LW} + \gamma_i^{AB} \quad (2)$$

The acid-base polar component  $\gamma_i^{AB}$  can be further subdivided by using specific terms for an electron donor ( $\gamma_i^-$ ) and an electron acceptor ( $\gamma_i^+$ ) subcomponent:

$$\gamma_i^{AB} = 2\sqrt{\gamma_i^+ \gamma_i^-} \quad (3)$$

The solid/liquid interfacial energy is then given by:

$$\gamma_{SL} = \gamma_S + \gamma_L - 2(\sqrt{\gamma_S^{LW} \cdot \gamma_L^{LW}} + \sqrt{\gamma_S^+ \cdot \gamma_L^-} + \sqrt{\gamma_S^- \cdot \gamma_L^+}) \quad (4)$$

Combining this with the Young equation (1), a relation between the measured contact angle and the solid and liquid surface free energy terms can be obtained:

$$\gamma_L \cdot (1 + \cos \theta) = 2(\sqrt{\gamma_S^{LW} \cdot \gamma_L^{LW}} + \sqrt{\gamma_S^+ \cdot \gamma_L^-} + \sqrt{\gamma_S^- \cdot \gamma_L^+}) \quad (5)$$

In order to determine the surface free energy components ( $\gamma_S^{LW}$ ) and parameters  $\gamma_S^+$  and  $\gamma_S^-$  of a solid, the contact angles of at least three liquids with known surface tension components ( $\gamma_L^{LW}$ ,  $\gamma_L^+$ ,  $\gamma_L^-$ ), two of which must be polar, have to be determined.

## 2.4 Bacterial adhesion

In this investigation, *Escherichia coli* (*E. coli*) JMI09 from the Wellcome Trust Bio-Center of the University of Dundee were used for bacterial adhesion tests. The strain was subcultured and preserved in 15% glycerol in TSB (Tryptone Soya Broth, Oxoid®, UK) as frozen stock at –80 °C. For all adhesion tests, TSA (Tryptone Soya Agar) plates were streaked out with a loop from the frozen stock and grown overnight at 37 °C. A single colony was inoculated in 20 ml TSB and grown statically overnight at 37 °C. Five hundred microlitres from this culture were further inoculated into 100 ml TSB in a conical flask and grown in a shaker-incubator at 37 °C and 250 rpm. The culture was grown to mid-exponential phase. The strains were harvested by centrifugation at 4500 rpm for 5 min at –4 °C, washed once in sterile distilled water and re-suspended in the medium (pre-warmed to 37 °C) at a 10<sup>7</sup> CFU/ml concentration.

The samples were put in a sterile beaker with 100 ml bacterial suspension (10<sup>7</sup> CFU/ml) and incubated at 37 °C for 1h under a gentle stirring at 20 rpm in a shaker incubator (Stuart Scientific, UK). Each sample was taken from the suspension using sterile forceps and was gently dipped into warm, sterile distilled water under a constant detachment

force by a detachment instrument to remove loosely bound bacteria, then transferred to a sterile glass beaker with 3 ml pre-warmed sterile distilled water. The bacteria adhered to the surface was removed from the surface by sonication for 10 min. One hundred microlitres of the sonication suspension and  $10^{-1}$ ,  $10^{-2}$  and  $10^{-3}$  dilutions were plated out on TSA plates (two plates for each concentration) and incubated overnight at 37 °C. The colonies were counted on the following day.

### 2.5 CaSO<sub>4</sub> deposit formation

Fouling tests were carried out in a pool boiling test rig at atmospheric pressure, which is similar to a water kettle. The rig contained 1.2 g/l CaSO<sub>4</sub> solution. The heaters were coated with Ni-P-PTFE with various surface energies. An untreated heater was used as control. The heat flux of the heater was 100 kW/m<sup>2</sup>. The CaSO<sub>4</sub> deposit which formed on each heater rod for a given heating time was removed. The deposit was dried and weighted using a Sartorius electronic scale with 10<sup>-5</sup> g precision. Then the weight of the deposit per centimetre square heater surface was calculated.

### 2.6 Protein adhesion

In this investigation 10 mm q-sense discs were coated with Ni-P-PTFE with various surface energies using electroless plating technique. Bovine fibrin was used in the experiment. The protein solution was prepared at the concentrations of 20 µg/ml by solving 0.9% NaCl sterile distilled water and centrifuged at 4500rpm at 4 °C for 5 minutes. Protein adhesion was measured with a Quartz Crystal Microbalance (QCM-D300).

## 3. RESULTS

### 3.1 Surface energy of Ni-P-PTFE

The surface energy of Ni-P-PTFE coatings was changed in the range of 20-40 mN/m, depending on PTFE content in the coatings. The surface energies of stainless steel, Ni-P coating, Ni-P-PTFE with 2% PTFE, Ni-P-PTFE with 20% PTFE and Ni-P-PTFE with 28% PTFE were 39.6, 34.9, 27.5, 24.1 and 21.0 mN/m, respectively.

### 3.2 Bacterial adhesion

Fig.1 shows the effect of the surface energy of the coatings and stainless steel 304 on the attachment of *E.coli* JM109 for contact time 5 hours at 37°C. The number of cell colonies attached to untreated stainless steel surface was around  $5.0 \times 10^5$  CFU/cm<sup>2</sup>. The number of cell colonies attached to the Ni-P and Ni-P-PTFE coated surfaces was in the range  $4.0 \times 10^4$  -  $6.1 \times 10^4$  CFU/cm<sup>2</sup>. The Ni-P-PTFE coating with surface energy 27.5 mN/m performed best in inhibiting bacterial adhesion.

### 3.3 CaSO<sub>4</sub> deposit formation

Fig. 2 shows that the surface energy of the coatings had a significant influence on the adhesion of CaSO<sub>4</sub> deposits.

When the surface energy of the coatings was around 28 mN/m, the adhesion of CaSO<sub>4</sub> deposits was minimal.

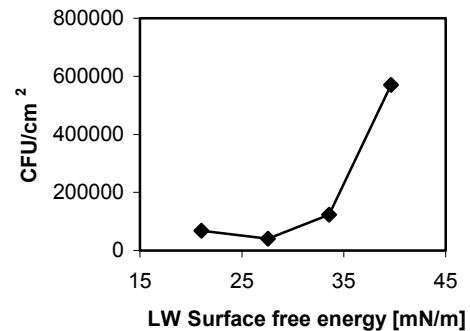


Fig. 1 Effect of the LW surface energy on *E.coli* JM109 attachment for contact time 5 hours at 37°C

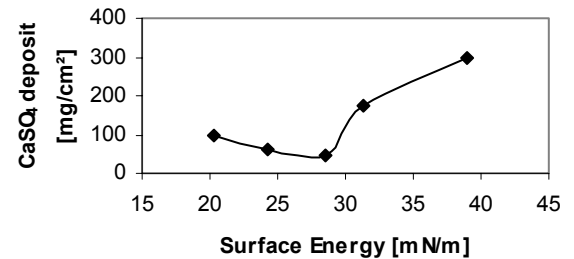


Fig. 2 Effect of the surface energy of the coatings on the adhesion of CaSO<sub>4</sub> deposits

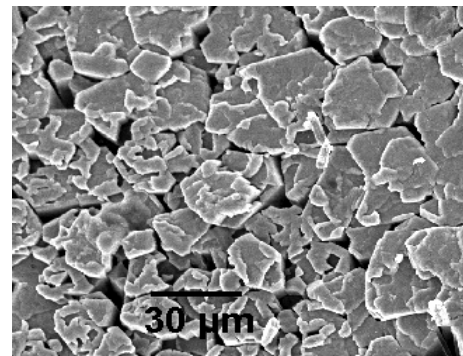


Fig. 3 Bare surface with surface energy 39.6 mN/m

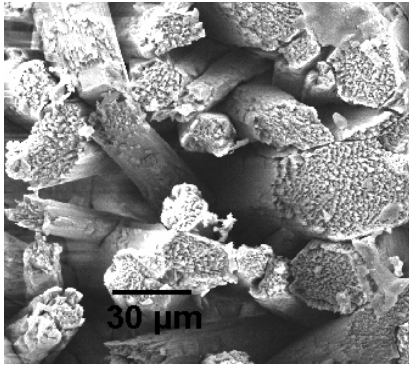


Fig. 4 Ni-P-PTFE coated surface with surface energy 28 mN/m

Figs. 3 and 4 show the effect of the surface energy of the coatings on the microstructure of  $\text{CaSO}_4$  deposits. Fig. 3 shows that the deposit formed on the bare surface with surface energy 39.6 mN/m exhibits a packed structure. The density of the deposit on the bare surface was  $2.9 \text{ g/cm}^3$ . The deposits formed on the Ni-P-PTFE coated surfaces with surface energy 28 mN/m exhibit a loose and porous structure with no defined orientation, as shown in Fig 4. The corresponding deposit density was only  $1.0 \text{ g/cm}^3$ .

### 3.4 Protein adhesion

The experimental results show that the adsorption causes an initial rapid frequency decrease (mass increase) for bovine fibrin, followed by a slower frequency decrease as the surface coverage saturates. Figs 5 and 6 show the effect of surface energy on the adsorption of bovine fibrin.

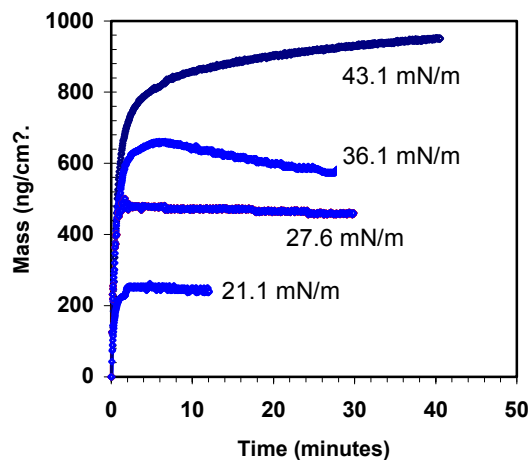


Fig 5 Adsorption of bovine fibrin with time on substrates with different surface energies

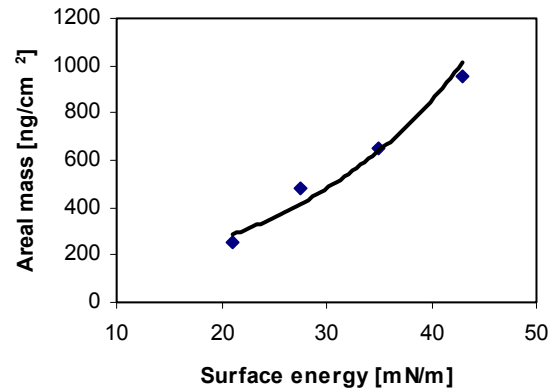


Fig 6 Effect of surface energy on the adsorption of bovine fibrin

Obviously the surface energy of the surfaces have a significant influence on the protein adsorption. The adsorption of bovine fibrin decreased with the surface energy decreasing. The experimental results indicate that Ni-P-PTFE surface with surface energy 21.1 mN/m performed best in inhibiting prion protein adhesion, compared with stainless steel 304 and other surfaces. The proteins were removed easily from the Ni-P-PTFE coated surface, and no protein residual was observed with SEM after cleaning. While some protein residual was observed on stainless steel surfaces after cleaning under identical conditions.

## 4. DISCUSSION

Fouling adhesion may be described with the extended DLVO (Deryagin, Landau, Verwey and Overbeek) theory (van Oss, 1994). According to this theory, the principal interaction forces determining hetero-coagulation include a Lifshitz-van der Waals (LW) interaction component, an electrostatic double-layer (EL) component, a Lewis acid-base (AB) component, and Brownian motion (Br) (van Oss, 1994). The total interaction energy  $\Delta E_{132}^{TOT}$  between particle (1) and a solid surface (2) in a fluid (3) can be written as the sum of these corresponding interaction terms (van Oss, 1994; Oliveira, 1997):

$$\Delta E_{132}^{TOT} = \Delta E_{132}^{LW} + \Delta E_{132}^{AB} + \Delta E_{132}^{EL} + \Delta E_{132}^{Br} \quad (6)$$

The balance between all possible interactions determines whether or not the bacteria will attach on the surface: adhesion will take place when  $\Delta E_{132}^{TOT}$  is negative (i.e. total interaction force is attractive) (Oliveira, 1997).

Recently, Zhao and Müller-Steinhagen (2002) derived the optimum surface free energy components of a surface, for which bacterial adhesion force is minimal, using the extended DLVO theory:

$$\gamma_S^{TOT} = \frac{1}{4} \cdot (\sqrt{\gamma_1^{LW}} + \sqrt{\gamma_3^{LW}})^2 \quad (7)$$

As the equation isolates the effect of surface free energy upon particulate adhesion from the numerous parameters in the extended DLVO theory, it appears relatively simple.

Equation (7) explains the experimental results – why bacterial adhesion was minimal when the LW surface free energy of the coatings was about 27.5 mN/m. The  $\gamma_1^{LW}$  value of *E. coli* JM109 was 35.6 mN/m and  $\gamma_3^{LW}$  of water was 21.8 mN/m. Equation (7) then produces a theoretical value of  $\gamma_S^{TOT} = 28.2$  mN/m, which approximates the experimental value of the surface free energy for which *E. coli* attachment was minimal. According to Förster and Bohnet (2002), the average LW surface free energy of CaSO<sub>4</sub> deposits,  $\gamma_1^{LW}$  was around 37 mN/m, and the  $\gamma_3^{LW}$  of water is 21.8 mN/m. Equation (7) then produces a surface free energy value  $\gamma_S^{TOT} = 29$  mN/m, which approximates the experimental value of the surface free energy (28 mN/m) for which the precipitation of CaSO<sub>4</sub> salt on heat transfer surfaces was minimal. For protein adhesion, a similar conclusion was obtained.

In addition to surface free energy, other factors, including surface charge, surface roughness, temperature, contact time and fluid flow velocity also have significant influence on bacterial or CaSO<sub>4</sub> adhesion and growth (Ritter and Sutor, 1975; and Karabelas, 2002). Therefore, the mechanisms of bacterial adhesion or CaSO<sub>4</sub> adhesion are complex. If, however, initial bacterial or CaSO<sub>4</sub> adhesion strength is reduced by an optimal surface free energy approach, they could be removed easily from the surfaces by flowing water. This may lead to a way of controlling biofouling or mineral fouling formation.

## CONCLUSIONS

- 1) The surface free energy of Ni–P–PTFE coatings decreased with increasing PTFE content in the coatings.
- 2) The number of cell colonies attaching to the surfaces with various surface energies decreased with decreasing surface free energies until coating surface energy reached to 28 mN/m.

- 3) The surface free energy of the Ni–P–PTFE coated surfaces has a significant influence on CaSO<sub>4</sub> deposit adhesion. When the surface free energy of the Ni–P–PTFE coated surfaces was in the range 28–30 mN/m, the adhesion of CaSO<sub>4</sub> deposit was minimal.
- 4) The surface free energy of the Ni–P–PTFE coated surfaces has a significant influence on protein adhesion. The mass of protein attaching to the surfaces with various surface energies decreased with decreasing surface free energies.

## NOMENCLATURE

$\Delta E$	Interaction energy, J
$\theta$	Contact angle, °
$\gamma$	Surface tension or surface free energy; mN/m

## Subscript

1	Bacteria or crystal
2	Solid surfaces, coatings
3	Media, water
L	Liquid
S	Surface

## ACKNOWLEDGEMENTS

The part of this work was supported by the EU FP6 AMBIO project: 'Advanced Nanostructured Surfaces for the Control of Biofouling'.

## REFERENCES

- Förster, M., Bohnet, M., (2000). Modification of molecular interactions at the interface crystal/heat transfer surface to minimize heat exchanger fouling. *International Journal of Thermal Sciences* 39, 697-708.
- Gaffoglio, C.J., 1987, Beating biofouling with copper-nickel alloys offshore, *Sea Technology* Vol.28, pp. 43–46
- Karabelas, A.J., (2002). Scale formation in tubular heat exchangers-research priorities. *International Journal of Thermal Science* 41, 682-692.
- Koh, L.L., Hong, W.K. and Lip, L.K. 1991, Ecology of marine fouling organisms at eastern Johore strait, *Environmental Monitoring and Assessment*, Vol.19, pp. 319–333.
- Lalande, M., Rene, F. and Tissier, J.P. 1989, Fouling and its control in heat exchangers in the dairy industry, *Biofouling*, Vol. 1, pp. 233–250.
- Lucas, K.E., Bergh, J.O. and Christian, D.K. 1996, Dechlorination equipment development for shipboard

pollution prevention, *Naval Engineers Journal*, Vol.108, pp. 19–25

Müller-Steinhagen, H. and Zhao, Q. 1997, Investigation of low fouling surface alloys made by ion implantation technology, *Chemical Engineering Science*, Vol.52, pp. 3321–3332.

Notermans, S., Dormans, J.A.M.A. and Mead, G.C. 1991, Contribution of surface attachment to the establishment of microorganisms in food processing plants: a review, *Biofouling*, Vol. 5, pp. 21–36.

Oliveira, R., (1997). Understanding adhesion: a means for preventing fouling. *Experimental Thermal and Fluid Science* 14, 316-322.

Ritter, R.B., Sutor, J.M., 1975. Handling and disposal of solid. Proceedings of the Second NATL Conference on Complete Water Reuse. Water's Interface with Energy, Air and Solids, Chicago, IL, 604–609.

Tulsi, S.S. 1983, Composite PTFE–nickel coatings for low friction applications, *Finishing*, Vol.7, pp. 14–18.

van Oss, C.J. (1994). *Interfacial Forces in Aqueous Media*. Marcel Dekker, New York.

van Oss, C.J., Good, R.J., Chaundhury, M.K., (1988). Additive and nonadditive surface-tension components and the interpretation of contact angles. *Langmuir* 4, 884-891.

Young, T., (1805). An essay on the cohesion of fluids. *Philosophical Transactions of the Royal Society*, London 95, 65-87.

Zhao, Q., Müller-Steinhagen, H., (2002). Intermolecular and adhesion forces of deposits on modified heat transfer surfaces. in *Heat exchanger fouling – Fundamental Approches and Technical Solutions*, eds. H. Müller-Steinhagen et.al., Publico Publ., Essen, pp. 41-46.